Eur. Phys. J. B (2018) 91: 144
https://doi.org/10.1140/epjb/e2018-90295-1

THE EUROPEAN PHYSICAL JOURNAL B

Regular Article

On symmetric and asymmetric Van der Pol-Duffing oscillators

Vinícius Wiggers and Paulo C. Rech[a]

Departamento de Física, Universidade do Estado de Santa Catarina, 89219-710 Joinville, Brazil

Received 27 April 2018 / Received in final form 8 May 2018
Published online 2 July 2018

Abstract. We investigate numerically the dynamics of both symmetric and asymmetric Van der Pol-Duffing oscillators driven by a periodic force $F(t) = f\cos\omega t$. Each system is modeled by a different second order nonautonomous nonlinear ordinary differential equation controlled by five parameters. Our investigation takes into account the (ω, f) parameter-space in the two systems, keeping the other three parameters fixed. We verify the existence of parameter regions for which the corresponding trajectories in the phase-space are periodic, quasiperiodic, and chaotic, for the symmetric case. In the asymmetric case we verify the existence only of periodic and chaotic regions in the (ω, f) parameter-space. Finally, we also investigate the organization of the dynamics in the two systems, identifying Fibonacci and period-adding sequences of periodic structures.

1 Introduction

In this paper we investigate numerically the dynamics of two damped Van der Pol-Duffing forced oscillators, whose general mathematical form is given by [1–3]

$$\frac{d^2x}{dt^2} - \mu(1-x^2)\dot{x} + \frac{dV_i}{dx} = f\cos(\omega t), \tag{1}$$

where V_i $(i = 1, 2)$ is the potential function, f and ω are respectively the amplitude and the angular frequency of the external forcing, and μ is the damping parameter. Here we will consider a symmetric double-well potential function $V_1(x)$ given by

$$V_1(x) = \frac{\beta x^2}{2} + \frac{\alpha x^4}{4}, \tag{2}$$

and an asymmetric double-well potential function $V_2(x)$ given by

$$V_2(x) = \frac{\beta x^2}{2} + \frac{\alpha x^4}{4} + \frac{x^3}{3}, \tag{3}$$

where β and α are parameters. Both functions are depicted in Figure 1, with $\beta = -1$ and $\alpha = 1$ kept fixed. The symmetric case is represented by the red line, and the asymmetric case by the blue line.

Symmetric and asymmetric Van der Pol-Duffing oscillators, with the most varied types of forcing, have a wide utility in many fields, with consequent application to model several different nonlinear processes. Some few examples include the modeling of the stochastic response of a vibroimpact system under additive colored noise excitation [4], and optical bistability in a dispersive medium [5]. Van der Pol-Duffing oscillators can be properly coupled, with the resulting systems being useful to model electroencephalogram signals [6] and microelectromechanical systems resonators [7], which have significant use as sensors, biomedical implants, and wireless communication devices.

Our main goal in this work is to investigate the two-dimensional (ω, f) parameter-space of the forced Van der Pol-Duffing system (1), delimiting regions of different dynamical behavior for both cases, namely the one that considers the symmetric potential $V_1(x)$ in equation (2), and the one where is considered the asymmetric potential $V_2(x)$ in equation (3). The dynamical behavior of a very large number of points in the (ω, f) parameter-space, more exactly one million points, will be characterized for each of the two cases, for $\beta = -1$, $\alpha = 1$, and $\mu = 0.5$. In other words, each point in the (ω, f) parameter-space will have its related trajectory in the phase-space characterized as regular (periodic or quasiperiodic) or chaotic. With this purpose, both parameters ω and f are simultaneously varied in each case, system (1) is numerically integrated for each pair (ω, f), and Lyapunov exponents are sequentially calculated. Finally, the results obtained by considering the symmetric and the asymmetric potential functions are compared.

The paper is organized as follows. In Section 2 we present numerical results related to the organization of the dynamics in the (ω, f) parameter-space of system (1) for the symmetric Van der Pol-Duffing system. The asymmetric case is considered in Section 3, while concluding remarks are given in Section 4.

[a] e-mail: paulo.rech@udesc.br

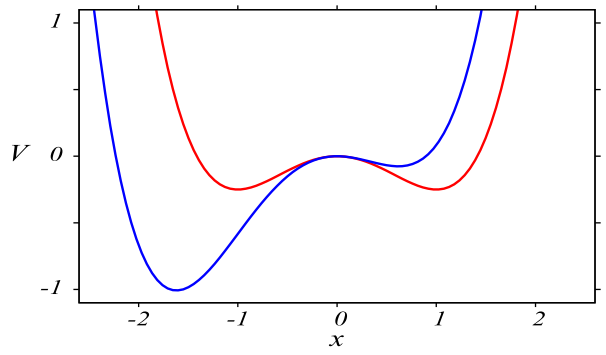

Fig. 1. Symmetric (red line) and asymmetric (blue line) double-well potential functions, obtained respectively from equations (2) and (3) with $\beta = -1$ and $\alpha = 1$.

2 The (ω, f) parameter-space of a symmetric Van der Pol-Duffing oscillator

Figures 2a and 2b show a global view of the (ω, f) parameter-space of a forced symmetric Van der Pol-Duffing oscillator, for $0 \leq \omega \leq 5$, $0 \leq f \leq 10$, and with $\mu = 0.5$ kept fixed. They were obtained by considering the symmetric potential $V_1(x)$ when $\beta = -1$, $\alpha = 1$, meaning that we are dealing with the symmetric double-well potential function plotted in Figure 1, namely that represented by the red line.

Numerical estimates of Lyapunov exponents spectra (LES) were used to obtain the diagrams in Figure 2. Each point, in each parameter-space, was painted according to the dynamical behavior presented, which was characterized by the related LES. Thus, a chaotic region, for which the largest Lyapunov exponent (LLE) is greater than zero, and the second LLE is equal to zero, is related to the same region that appears painted in yellow-red in Figure 2a, and in black in Figure 2b, with the same interpretation being given for the sets of diagrams in Figures 2c and 2d, and in Figures 2e and 2f. A periodic region, for which the LLE is equal to zero and the second LLE is less than zero, is related with a same region painted in black and grey, respectively in diagrams of Figures 2a and 2b, with the same interpretation being applied also to diagrams in Figures 2c and 2d, and in Figures 2e and 2f. A quasiperiodic region, for which the LLE and the second LLE are both equal to zero, is corresponding to a same region painted in black in the two diagrams of each of the three sets defined above. We would like to point out that this color code is also observed for all similar parameter-spaces throughout this text.

Before proceeding, we give details of the procedure for obtaining the diagrams in Figure 2. All of them, as well as all similar diagrams further on in this text, were obtained by computing LES in square grids of $10^3 \times 10^3$ parameters. System (1) was always integrated from the same initial condition, by using a fourth-order Runge–Kutta algorithm with a fixed time step equal to 10^{-3}, being discarded the first 1×10^6 integration steps, considered as a transient. To perform the computation of the average involved in the calculation of each one of the LES, were considered the next 1×10^6 integration steps.

Figures 2a and 2b allow us to see that, for a small amplitude of the external forcing, near to $f = 1$ in approximate values, the symmetric Van der Pol-Duffing forced oscillator is quasiperiodic in a wide range of the investigated angular frequency, namely for $1 \leq \omega \leq 5$. Embedded in the (ω, f) parameter-space, born in the quasiperiodic region (same region in black color in Figs. 2a and 2b) and extending to the chaotic region (same region in yellow-red color in Fig. 2a and black color in Fig. 2b), we can see organized periodic structures in black color in Figure 2a, which are similar to the Arnold tongues of the circle map [8]. Such periodic structures are better seen in the magnifications of the boxed regions A and B of Figure 2a, which are shown respectively in Figures 2c and 2e.

Note that some of the periodic structures in Figures 2c and 2e are labeled with a number which is related to the period of the respective structure. Period here is to be understood as the number of local maxima of the variable x, namely x_m, in one complete trajectory on the $(x, \dot{x})$ phase-space attractor. These periodic structures are usually depicted in conventional bifurcation diagrams like those shown in the plots of Figure 3, appearing in them as periodicity windows. Such diagrams help us to determine the periods of some structures, like those numbered in Figures 2c and 2e. Each bifurcation diagram in Figure 3 considers 10^3 values of the parameter ω, and was obtained by plotting the local maxima values of the variable x for each of them. Numerical integrations were performed under the same conditions as before in obtaining the parameter-spaces, then the local maxima were counted and plotted in the respective bifurcation diagram.

As can be seen in parameter-spaces depicted in diagrams of Figure 2, some type of organization of typical periodic structures (the Arnold tongues) is present. With regard to Figures 2c and 2e, as we move from right-hand to left-hand, along the straight line drawn in each of the diagrams, a same infinite set of periodic structures is crossed, which become smaller and smaller, and accumulate in the border of the large period-1 region in black at left. This set of periodic structures may be considered as being formed by two subsets of period-adding sequences, observed before in arrangements of other typical periodic structures, namely the shrimp-shaped periodic structures, in different continuous-time nonlinear mathematical models [9–19]. One subset is represented by the sequence $2 \to 3 \to 4 \to 5 \to 6 \to \ldots$, started at period-2 with an increase by a factor 1, while the other subset is represented by the sequence $3 \to 5 \to 7 \to 9 \to 11 \to \ldots$, this last sequence started at period-3, with an increase by a factor 2. In terms of the complete sequence, these periodic structures embedded in the quasiperiodic/chaotic region of Figures 2c and 2e are organized as $3 \to 2 \to 5 \to 3 \to 7 \to 4 \to 9 \to 5 \to \ldots$, whose general term is given by [20]

$$a_n = -\frac{1}{4}\left(-3 + (-1)^n\right)(n+2), \qquad n = 1, 2, 3, \ldots \quad (4)$$

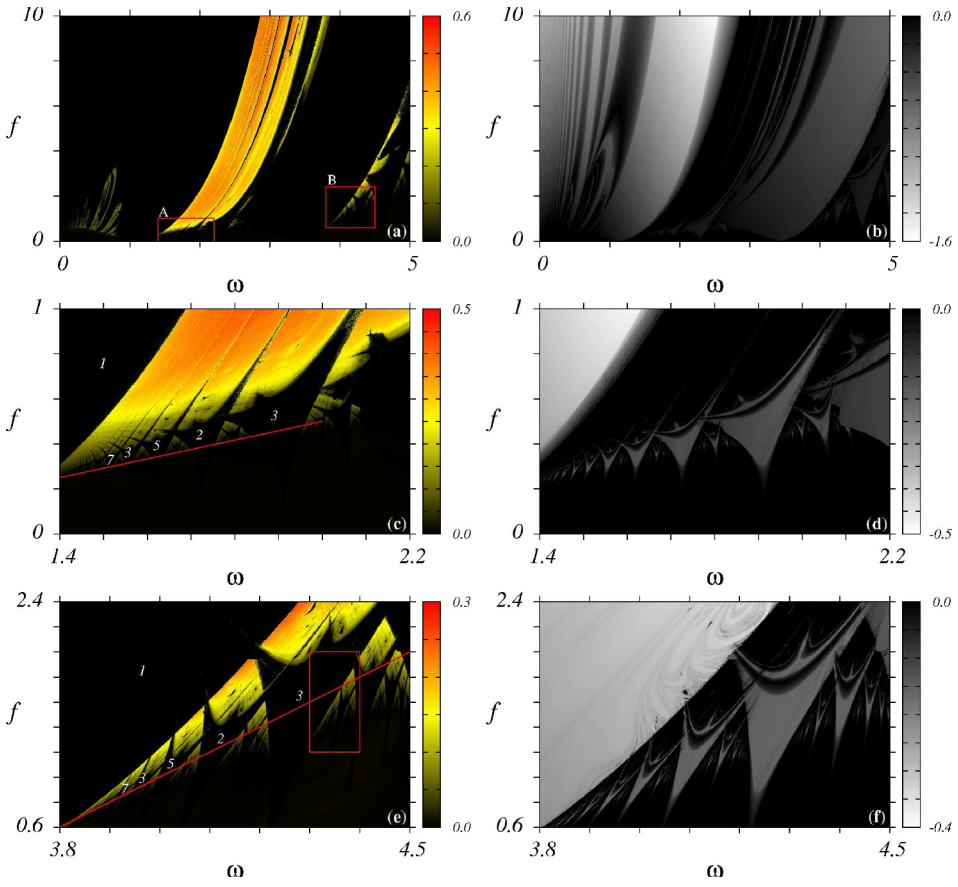

Fig. 2. Regions of different dynamical behaviors in the (ω, f) parameter-space of the forced symmetric Van der Pol-Duffing oscillator, according to estimates of the Lyapunov exponents spectra. Diagrams (a), (c), and (e) consider the largest Lyapunov exponent, while (b), (d), and (f) consider the second largest Lyapunov exponent. (a) and (b) Global view for $0 \leq \omega \leq 5$, $0 \leq f \leq 10$. (c) and (d) Magnification of the boxed region A in (a), where $1.4 \leq \omega \leq 2.2$, $0 \leq f \leq 1$. (e) and (f) Magnification of the boxed region B in (a), where $3.8 \leq \omega \leq 4.5$, $0.6 \leq f \leq 2.4$.

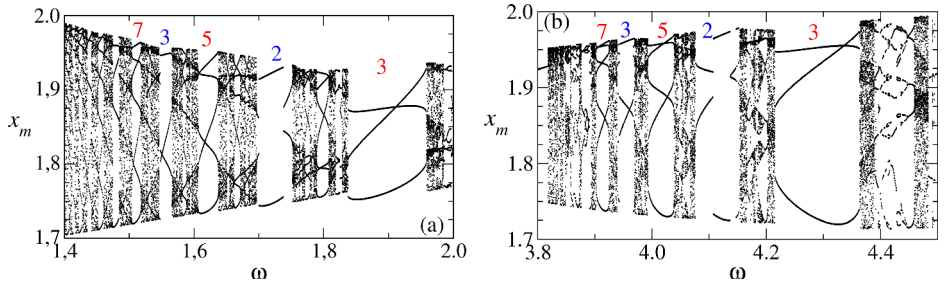

Fig. 3. Bifurcation diagrams for the forced symmetric Van der Pol-Duffing oscillator. Plotted is the number of local maxima of the variable x, as a function of the parameter ω. Numbers are related to periods. (a) Considering points along the straight line $f = 0.4166\omega - 0.3332$ drawn in Figure 2c. (b) Considering points along the straight line $f = 2\omega - 7$ drawn in Figure 2e.

It is important to note that the sequence (4) was derived based on numerical evidence detected in Figures 2c, 2e, 3a, and 3b. There is no analytical procedure for this purpose. In general, organization of regular and chaotic behaviors in parameter planes, needs to be obtained in an independent way, through numerical simulations considering the corresponding mathematical model.

Arrangements of periodic structures resulting in a sequence similar to that in (4), were before reported to a Hopfield-type neural network modeled by a set of three autonomous nonlinear first-order ordinary differential equations [21]. In this case, the periodic structures are shrimp-shaped, embedded in a chaotic region. Such typical periodic structures, shrimp-shaped, also appear with similar organization in a chaotic region of a periodically forced compound Korteweg-de Vries-Burgers system [22], which is modeled by a third-order partial differential equation. Boat-shaped periodic structures, and periodic structures similar to the Arnold tongues, are also present

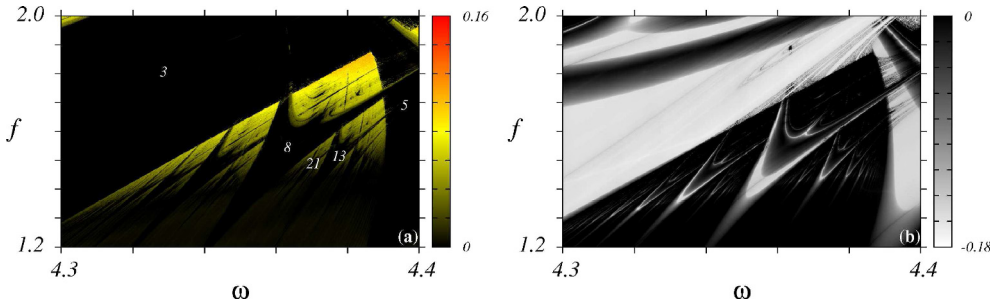

Fig. 4. Regions of different dynamical behaviors in the (ω, f) parameter-space of the forced symmetric Van der Pol-Duffing oscillator, according to estimates of the Lyapunov exponents spectra. Diagram (a) considers the largest Lyapunov exponent, while diagram (b) considers the second largest Lyapunov exponent. Both diagrams refer to magnification of the boxed region in Figure 2e, where $4.3 \leq \omega \leq 4.4$, $1.2 \leq f \leq 2.0$.

in this type of organization, in parameter planes of another damped-forced oscillator, modeled by a different second-order ordinary differential equation [12].

We would like to point out that the Arnold tongues present in the (ω, f) parameter-space of system (1) have self-similar properties. This is evidenced in Figures 2c and 2e, where it can be seen the presence of tongues in different length scales, between every two tongues belonging to any of the period-adding sequences seen before. Figure 4a shows a magnification of the boxed region in Figure 2e, for $4.3 \leq \omega \leq 4.4$, $1.2 \leq f \leq 2.0$, and following we will investigate the organization of periodicities of some tongues shown there.The largest tongue between period-3 and period-5 tongues is a period-8 tongue. Note that 8 is the sum of 3 and 5. The largest tongue between period-5 and period-8 tongues is a period-13 tongue, 13 being the result of the sum of 5 and 8. The largest tongue between period-8 and period-13 tongues is a period-21 tongue, 21 being the result of the sum of 8 and 13. This behavior is recurrent, and the result is the sequence of numbers (periods) $3 \to 5 \to 8 \to 13 \to 21 \to 34 \to \ldots$, clearly illustrated in Figure 4a. This time there is another type of organization of the tongues, again based on their respective periods. The rule followed for writing the sequence of numbers above considers that the period of a tongue in a certain position, is the difference of periods of both the subsequent and the previous tongues. Therefore, the number 5 in the position 2 of the sequence, related to the period-5 tongue, is the difference between 8 and 3, which are numbers related respectively to both period-8 and period-3 tongues. The period-8 tongue in the position 3 of the sequence, is the difference between 13 and 5, which are numbers related respectively to both period-13 and period-5 tongues, and so on.

The sequence $3 \to 5 \to 8 \to 13 \to 21 \to 34 \to \ldots$, generated by considering the periods of a set of Arnold tongues present in the (ω, f) parameter-space of the forced symmetric Van der Pol-Duffing oscillator, is similar to the Fibonacci sequence [23], in the sense that both sequences obey the same law of formation. As a consequence, the growth rate of the period in the sequence obtained here, given by P_{n+1}/P_n, with n being an integer signifying the position of each number in the sequence, converges to the golden ratio $\phi = (1 + \sqrt{5})/5 \approx 1.61803398$. To illustrate, $34/21 = 1.6190476\ldots$ is the ratio between periods of tongues at positions 6 and 5 in the sequence, while $987/610 = 1.6180328\ldots$ is the ratio between periods of tongues at positions 13 and 12. We emphasize that sequences similar to the above may be found between every two neighboring tongues, belonging to any of the sequences investigated before, and depicted in Figures 2c and 2e.

3 The (ω, f) parameter-space of an asymmetric Van der Pol-Duffing oscillator

Figures 5a and 5b show a global view of the (ω, f) parameter-space of a forced asymmetric Van der Pol-Duffing oscillator, for $0 \leq \omega \leq 5$, $0 \leq f \leq 10$, and with $\mu = 0.5$ kept fixed. They were obtained by considering the asymmetric potential $V_2(x)$ when $\beta = -1$, $\alpha = 1$, meaning that we are dealing with the asymmetric double-well potential function plotted in Figure 1, namely that represented by the blue line. As before in Figures 2 and 4, diagrams in Figure 5 were obtained by using numerical estimates of LES to characterize the dynamical behavior of each point. It is therefore possible to conclude that the system under study does not present quasiperiodic behavior, since common regions painted in black are not observed in any of the two sets of diagrams ((a)–(b), and (c)–(d)) in Figure 5.

The quasiperiodic region observed in the symmetric Van der Pol-Duffing forced oscillator investigated in Section 2, which as we have seen before is present in a wide range of the angular frequency, for a small amplitude of the external forcing, is this time, in the asymmetric case, replaced by a periodic region. As a consequence of the extinction of the quasiperiodic region when we switch from the symmetric to asymmetric case, organized periodic structures similar to the Arnold tongues of the circle map [8] are not observed in the forced asymmetric Van der Pol-Duffing oscillator. Therefore, the quasiperiodic behavior is extinguished by the asymmetry imposed by the potential function $V_2(x)$

Figure 5c, which is a magnification of the boxed region in Figure 5a, shows another kind of typical periodic structures, namely the shrimp-shaped periodic structures [24],

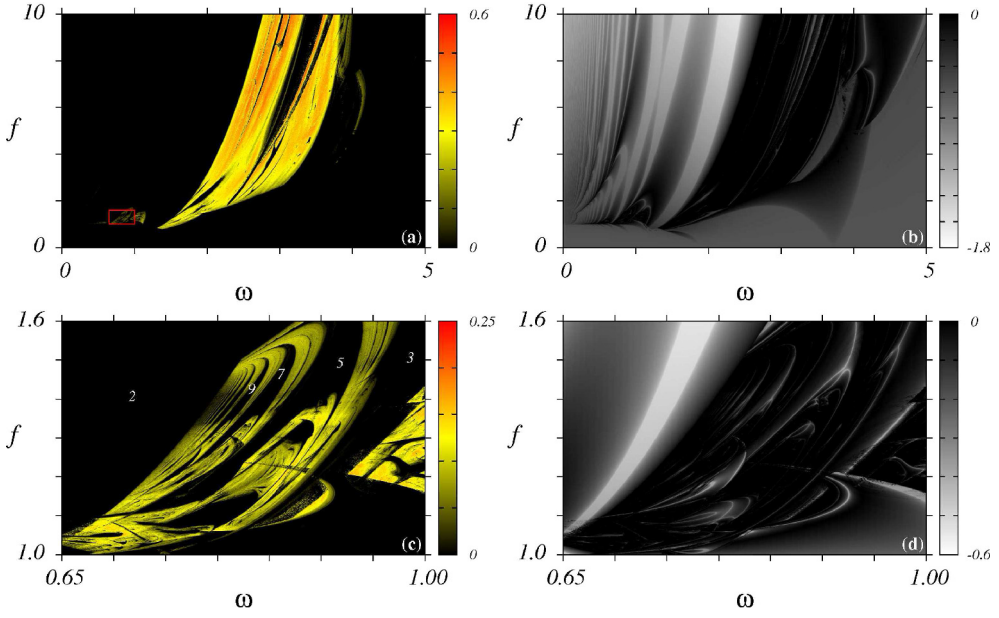

Fig. 5. Regions of different dynamical behaviors in the (ω, f) parameter-space of the forced asymmetric Van der Pol-Duffing oscillator, according to estimates of the Lyapunov exponents spectra. Diagrams (a) and (c) consider the largest Lyapunov exponent, while (b) and (d) consider the second largest Lyapunov exponent. (a) and (b) Global view for $0 \leq \omega \leq 5$, $0 \leq f \leq 10$. (c) and (d) Magnification of the boxed region in (a), where $0.65 \leq \omega \leq 1.00$, $1.0 \leq f \leq 1.6$.

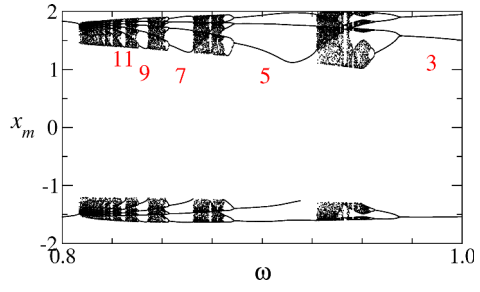

Fig. 6. A bifurcation diagram for the forced asymmetric Van der Pol-Duffing oscillator. Plotted is the number of local maxima of the variable x, as a function of the parameter ω. Numbers are related to periods. It was obtained by considering points along the horizontal straight line $f = 1.45$ not drawn in Figure 5c, for $0.8 \leq \omega \leq 1.0$.

whose organization this time occurs embedded exclusively in the chaotic region of the (ω, f) parameter-space of the forced asymmetric Van der Pol-Duffing oscillator. As before in Section 2, in the symmetric case, numbers labeling some periodic structures in Figure 5c, meaning the respective periods, were copied of the bifurcation diagram in Figure 6, which was obtained in a manner analogous to those diagrams in Figure 3. This time were considered points along the horizontal straight line $f = 1.45$, not drawn in Figure 5c because it is visually easy to locate. Note that as we move along this not drawn line in Figure 5c, from the right side to the left side, we detect a set of infinite periodic structures in black, numbered as 3, 5, 7, 9, 11,. . ., which are separated by chaotic regions in yellow to red, while get smaller and smaller and accumulate in the border of the period-2 black region at left. Such periodic structures constitute a part of a period-adding sequence $3 \to 5 \to 7 \to 9 \to 11 \ldots$, where the periodicity is increased by a constant factor equal to 2, as the parameter ω decreases. Note that the period of the accumulation region, namely 2, is equal to the growth rate of the sequence. This behavior in a two-dimensional parameter-space, where typical periodic structures separated by chaotic regions, are organized in sequences whose period of the next structure is increased by a constant number equal to the period of the accumulation region, was observed before in several other different continuous-time mathematical models of real systems [9–14].

4 Summary

In this paper we report on the nonlinear dynamics of symmetric and asymmetric Van der Pol-Duffing oscillators driven by a same periodic force $F(t) = f \cos \omega t$. For each of the systems we have investigated a two-dimensional parameter-space, namely that considering the angular frequency ω and the amplitude f of the external forcing. Regardless of the case under consideration, symmetric or asymmetric, we have verified a certain organization of the dynamics in the two systems, in the (ω, f) parameter-space.

Both systems show regions for which the corresponding trajectories in the phase-space are periodic or chaotic. Quasiperiodic regions are also observed, but only in the symmetric case. We also investigate the organization of the dynamics in the two systems, showing the existence of typical periodic structures embedded in chaotic regions, the so-called shrimps, organized in period-adding sequences in the asymmetric case. Finally, we have shown

the existence of other typical periodic structures, the Arnold tongues, born in the quasiperiodic region and extending to the chaotic region of the symmetric case, whose periods are organized as in a Fibonacci sequence.

The authors thank Conselho Nacional de Desenvolvimento Científico e Tecnológico-CNPq, and Fundação de Amparo à Pesquisa e Inovação do Estado de Santa Catarina-FAPESC, Brazilian Agencies, for financial support.

Author contribution statement

This work was carried out in collaboration between both authors. Both authors performed the computations. Results were discussed by both authors. Author PCR wrote the first version of the manuscript. Both authors revised the manuscript and approved this version.

References

1. J. Cui, J. Liang, Z. Lin, Phys. Scr. **91**, 015201 (2016)
2. V. Wiggers, P.C. Rech, Chaos Soliton Fract. **103**, 632 (2017)
3. A.J. Brizard, M.C. Westland, Commun. Nonlinear Sci. Numer. Simulat. **43,** 351 (2017)
4. C. Li, W. Xu, L. Wang, D.X. Li, Chin. Phys. B **22**, 110205 (2013)
5. Y.H. Kao, C.S. Wang, Phys. Rev. E **48**, 2514 (1993)
6. P. Ghorbaniana, S. Ramakrishnana, A. Whitmanb, H. Ashrafiuona, Biomed. Signal Process. Control **15**, 1 (2015)
7. A. Kumar, P. Mohanty, Sci. Rep. **7,** 411 (2017)
8. H.G. Schuster, W. Just, *Deterministic Chaos an introduction* (Wiley-VCH, Weinheim, 2005)
9. H.A. Albuquerque, R.M. Rubinger, P.C. Rech, Phys. Lett. A **372**, 4793 (2008)
10. C. Bonatto, J.A.C. Gallas, Phys. Rev. E **75**, 055204 (2007)
11. T.S. Krüger, P.C. Rech, Eur. Phys. J. D **66**, 12 (2012)
12. F.G. Prants, P.C. Rech, Eur. Phys. J. B **87**, 196 (2014)
13. P.C. Rech, Int. J. Bifurc. Chaos **25**, 1530035 (2015)
14. P.C. Rech, Phys. Scr. **91,** 075201 (2016)
15. S.L.T. de Souza, A.M. Batista, M.S. Baptista, I.L. Caldas, J.M. Balthazar, Physica A **466**, 224 (2017)
16. P.C. Rech, Phys. Scr. **92,** 045201 (2017)
17. P.C. Rech, Eur. Phys. J. B **90**, 251 (2017)
18. M. Borghezan, P.C. Rech, Chaos Soliton Fract. **97**, 15 (2017)
19. V. Wiggers, P.C. Rech, Int. J. Bifurc. Chaos **27**, 1730023 (2017)
20. http://www.wolframalpha.com
21. A.C. Mathias, P.C. Rech, Neural Networks **34**, 42 (2012)
22. P.C. Rech, Eur. Phys. J. B **86**, 356 (2013)
23. R.A. Dunlap, *The golden ratio and Fibonacci numbers* (World Scientific, Singapore, 2003)
24. J.A.C. Gallas, Phys. Rev. Lett. **70,** 2714 (1993)